Appl. Phys. B 58, 243–248 (1994)

Applied Physics B Lasers and Optics

Optical Parametric Processes and Broadly Tunable Femtosecond Sources

C. L. Tang, P. E. Powers, R. J. Ellingson

Cornell University, Ithaca, NY 14853, USA

Received 14 September 1993/Accepted 24 November 1993

Abstract. The basic concepts of optical parametric processes and recent results on broadly tunable high-repetition rate femtosecond Optical Parametric Oscillators (fs OPO) are reviewed. Ti:Sapphire-Laser pumped KTP, KTA, and CTA fs OPOs and intracavity-doubled fs KTP OPO in particular are discussed.

PACS: 42.65.Re

In the development of tunable femtosecond sources, to achieve broad tunability without scarificing time resolution is a well recognized goal. The need to achieve these at sufficiently high pulse-repetition rate is not, however, often emphasized. Yet, in the study of ultrafast relaxation processes, as the time resolution increases, more details of the relaxation dynamics will inevitably be revealed, including the possibility of multiple or stretched exponential processes. To analyze the data from the usual pump-probe type of experiments in such studies, more sophisticated methods [1] are needed beyond simple graphic methods such as drawing asymptotes to a single decay curve, which is notoriously inadequate when more than one or two simple exponentials are involved. These sophisticated methods require highly accurate data. Higher pulse-repetition rate leads to higher signal-to-noise ratio and, in turn, more accurate data. Thus, there is a need to achieve broad tunability, short pulse width, and sufficiently high repetition rate at the same time. These requirements can be met simultaneously at reasonable power levels only in a femtosecond Optical Parametric Oscillator (fs OPO), because of the following reasons. To achieve true broad continuous tunability, the device must be some sort of parametric device. To maintain the shortest possible pulse width, the parametric conversion crystal must be very thin to avoid group-velocity dispersion and to phasematch the entire femtosecond spectrum. For a thin parametric crystal, the single pass conversion efficiency will be low at the power levels of currently available high repetition rate pump sources because of the lack of high-power femtosecond amplifiers at high repetition rates. Thus, the parametric device must be an oscillator, not a single- or double-pass parametric amplifier. For optical parametric oscillators, the conversion efficiency can easily be in the range of 30% to 50% at a few times above the oscillation threshold.

The basic concept of the parametric process is of course not new [2–5], but the practical development of the devices had been very slow in coming due to the lack of suitable nonlinear optical materials. Progress in the development of a number of new nonlinear optical crystals in the past decade has finally led to the recent rapid advances in optical parametric devices. Since the earlier work on optical parametric oscillators, which never became practical due to the lack of suitable pump sources and nonlinear crystals, there have been considerable efforts on optical parametric amplifiers in the picosecond time domain. These tend to be synchronously pumped low-repetition rate single-pass optical parametric amplifiers [6] or pulsed oscillators [7]. The basic requirements for such parametric generators are very different from those for high-repetition rate oscillators in the short femtosecond time domain. Nevertheless, these earlier efforts are the precursors of the recent advances in the latter devices.

The first cw high-repetition rate femtosecond OPO was demonstrated by Edelstein et al. [8]. Because of the relatively low pump power from the high-repetition rate Rh 6G femtosecond dye lasers, the KTP OPO must be pumped within the cavity of the dye laser. Broadly tunable fs OPOs covering the spectral range from approximately 7000 Å to 3.5 μm have been demonstrated and used in experiments [9, 10]. However, to make such an intracavity device to oscillate is exceedingly difficult. It requires extraordinary precision in the alignment of all the optics in the coupled OPO and the dye laser cavities.

A breakthrough in the ease of operation of the KTP fs OPO came with the recent development of the relatively high powered femtosecond Ti:Sapphire laser [11]. Because the power level of such a laser can easily exceed the threshold of a KTP OPO at a couple of hundred mW, the fs OPO can now be pumped externally to the pump-laser cavity thus decoupling the optical alignment processes in

the pump laser and the OPO. With the power level of the mode-locked Ti:Sapphire lasers now approaching 3 W, there has been spectacular progress in the development of the fs OPO. Hundreds of mW at 10^8 Hz pulse-repetition rate and pulse width less than 100 fs can now be generated in Ti:Sapphire-Laser pumped KTP OPO in the wavelength range from 700 nm to 3.4 μm. With the newer nonlinear crystals such as KTA and CTA, the tuning range can be extended to the important 3 μm to 5 μm range. Extension to the still longer wavelength range of 10 μm is possible with $AgGaS_2$ and to the 20 μm range with $AgGase_2$. The field is still in its infancy. In this paper, we will first review the basic principles of the fs OPO. It will be followed by a brief report of some of the more recent results from our laboratory. Substantial efforts are also under way in a number of other laboratories to develop broadly tunable optical parametric sources in the picosecond and femtosecond time domain [12–14].

1 Basic Concepts

The parametric process is one of the most elementary nonlinear optical processes involving three photons and can be represented schematically by the simplest kind of Feynman diagram (Fig. 1). It describes the process in which one high-frequency photon is annihilated and two lower-frequency photons are created. This process has its origin in the second-order nonlinear polarization in the expansion of the induced macroscopic polarization **P** in the nonlinear medium in powers of the electric field **E** [cgs Gaussian units]:

$$\begin{aligned}\mathbf{P} &= \chi^{(1)}\mathbf{E} + \chi^{(2)}\mathbf{EE} + \chi^{(3)}\mathbf{EEE} + \ldots \\ &= \mathbf{P}^{(1)} + \mathbf{P}^{(2)} + \mathbf{P}^{(3)} + \ldots . \end{aligned} \tag{1}$$

This second-order polarization term, $\mathbf{P}^{(2)}$, leads to a term proportional to $\mathbf{E}^3$ in the Hamiltonian of the field in the medium:

$$H = H_0 + H_1 , \tag{2}$$

where H_0 is the field Hamiltonian corresponding to the medium in the absence of the nonlinearity:

$$H_0 = \frac{1}{8\pi}\int (\mathbf{D}\cdot\mathbf{E} + \mathbf{B}\cdot\mathbf{H})d\mathbf{r} . \tag{3}$$

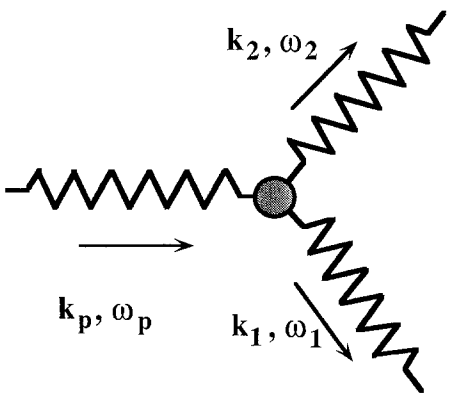

Fig. 1. Break down of a pump photon into a signal and an idler photon by the spontaneous parametric process

For optical parametric processes, the transparency region of the optical medium is of interest. The response of the medium to the fields can then be assumed local in space and time. For moderately strong fields, the total Hamiltonian can also be expanded in a Taylor series, as in the case of the induced poalrization in the medium. The corresponding interaction Hamiltonian H_1 describing the nonlinear response of the medium is, therefore, of the form:

$$H_1 = \tfrac{1}{3}\sum_{ijk}\int \chi^{(2)}_{ijk}E_i(\mathbf{r},t)E_j(\mathbf{r},t)E_k(\mathbf{r},t)\mathbf{dr} . \tag{4}$$

Quantizing the fields leads, in turn, to a term of the form $\chi^{(2)}\mathbf{a_1^-}\mathbf{a_2^+}\mathbf{a_3^-}$ in the interaction part of the Hamiltonian, where the $\mathbf{a}^+$'s and $\mathbf{a}^-$'s are the creation and annihilation operators, respectively, of the appropriate photons. This term corresponds to the parametric process in which a photon at ω_1 is annihilated to create two photons at ω_2 and ω_3.

In a three-photon parametric process, if the initial state, $|i\rangle$, of the field contains only N_1 pump photons in mode-1 at frequency ω_1 but no photon in mode-2 and mode-3 at frequencies ω_2 or ω_3, respectively, the correponding parametric process is the spontaneous parametric emission process through which one pump photon at ω_1 spontaneously breaks down into two lower-frequency photons at ω_2 and ω_3 in the final state $|f\rangle$, or:

$$|i\rangle = |N_1 0\,0\rangle \rightarrow |f\rangle \propto \sqrt{N_1}|(N_1-1)\,1\,1\rangle , \tag{5}$$

with the energy and momentum conserved:

$$\omega_1 = \omega_2 + \omega_3 , \tag{6}$$

and

$$\mathbf{k_1} = \mathbf{k_2} + \mathbf{k_3} . \tag{7}$$

In this case, the corresponding transition probability is proportional to N_1 or the intensity of the pump beam.

If there are already photons at ω_2 and ω_3 (which are also referred to as signal and idler frequencies ω_s and ω_i using the nomenclature borrowed from earlier microwave parametric oscillator work), then stimulated emission takes place, or:

$$\begin{aligned}|i\rangle = |N_1 N_2 N_3\rangle \rightarrow |f\rangle &\propto \sqrt{N_1(N_2+1)(N_3+1)} \\ &\times |(N_1-1)(N_2+1)(N_3+1\rangle , \end{aligned} \tag{8}$$

which shows that the transition probability to the final state is proportional to not only the intensity of the pump beam, but also those of the signal and idler beams. This means that the more the signal or idler photons that are present in the medium already, the more signal and idler photons will be emitted through this process. This is just like the stimulated emission process in ordinary lasers or masers. Here it corresponds to amplification of the signal and idler beams through amplification process.

The stimulated parametric process can be understood simply on the basis of classical coupled-wave equations for the signal and idler waves, assuming the parametric conversion to be small so that the pump field strength E_p can be assumed a constant parameter:

$$\left(\frac{\partial^2}{\partial z^2} + \frac{n_2^2\omega_2^2}{c^2}\right)E_2(z)e^{ik_2 z} = -\frac{4\pi\omega_2^2}{c^2}d_{\text{eff}}E_p E_3^* e^{ik_2 z} , \tag{9}$$

and

$$\left(\frac{\partial^2}{\partial z^2}+\frac{n_3^2\omega_3^2}{c^2}\right)E_3(z)\mathrm{e}^{\mathrm{i}k_3 z}=-\frac{4\pi\omega_3^2}{c^2}\,d_{\mathrm{eff}}E_{\mathrm{p}}E_2^*\mathrm{e}^{\mathrm{i}k_3 z}\,, \quad (10)$$

The effective Kleinmann d-coefficient is defined as:

$$d_{\mathrm{eff}}=\sum_{i,j,k=1}^{3}\chi^{(2)}_{ijk}\varepsilon_{pi}\varepsilon_{2j}\varepsilon_{3k}\,,$$

where ε_{ij} is the direction cosine of the E_i-field relative to the $\hat{j}$-axis. Further simplification of these equations on the basis of the slowly-varying-amplitude approximation leads to the coupled-amplitude equations and the parametric gain coefficient:

$$g=\frac{2\pi d_{\mathrm{eff}}|E_{\mathrm{p}}|\sqrt{k_2k_3}}{n_2n_3}\,. \quad (11)$$

The corresponding parametric tuning characteristics are determined by the energy conservation and phase-matching conditions (6) and (7), respectively.

For femtosecond OPOs, in addition to the phase-matching condition, the pump, signal, and idler pulses must overlap in the nonlinear crystal. Thus, the group-velocity dispersion in the nonlinear crystal limits the length of the crystal that can be used. For KTP pumped by a Ti:Sapphire laser, for example, the limiting length is on the order of a mm. With such a thin crystal, the pump beam must be tightly focused and well aligned [2,6] to reach the oscillation threshold and achieve optimum efficiency of the OPO. Typical pump intensity is on the order of a few hundred MW to GW/cm^2 resulting in a single-pass gain of a few %. Because of the low single-pass gain in the crystal, many passes around the cavity are required for the signal to build up from the noise due to the spontaneous parametric emission to the final steady-state level of the OPO; therefore, the tolerance on the cavity length must be tightly controlled to match the pump-pulse repetition rate.

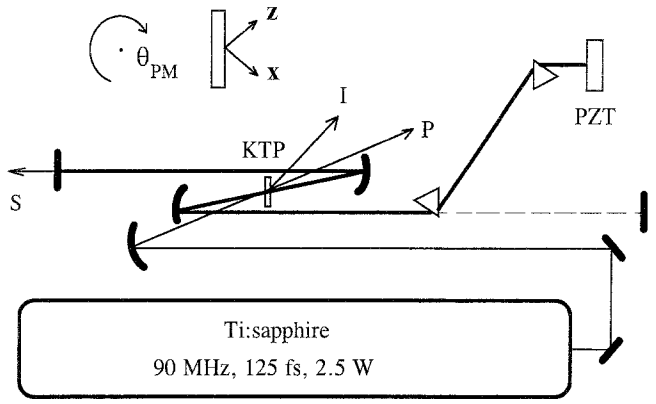

Fig. 2. Schematic of the OPO cavity in the vertical plane. The Ti:Sapphire pump is focused onto the 1.15 mm KTP crystal. An enlarged view of the crystal is depicted above and shows the orientation for Type-II phase matching at the angle θ_{PM}. The signal branch (S) is resonated by using a 1% output coupler and a PieZoelectric Transducer (PZT) for fine length adjustment. The idler (I) exits from the crystal at $\approx 6°$ from the signal. The prism sequence can be raised to allow oscillation without prisms

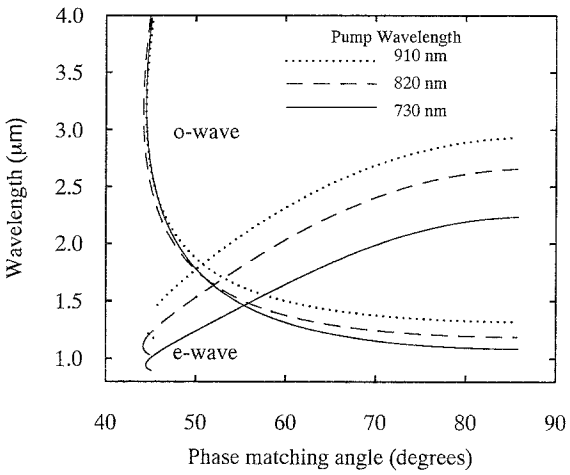

Fig. 3. Tuning curve of Ti:Sapphire laser pumped Type-II phase-matched KTP femtosecond OPO

2 Broadly Tunable Femtosecond Sources

2.1 Ti:*Sapphire-Laser-Pumped Femtosecond* OPOs

A schematic of a typical Ti:Sapphire-laser pumped KTP OPO [15] is shown in Fig. 2. The arrangement is straightforward and much simpler to operate in comparison with the intracavity pumped fs OPO [8–10]. The intracavity prisms are important for group-velocity dispersion compensation. Without these intracavity prisms, the pulses tend to be strongly chirped which cannot be compensated with external prisms. A clear example is the experiment reported in [16], where strong chirping of the pulses extends over several hundred fs even though the coherent peak has a sub-100 fs width.

Tuning curves of the Ti:Sapphire-Laser pumped Type-II (o$\rightarrow$e+o, to take advantage of the larger d_{eff} for KTP) phase-matched KTP OPO are shown in Fig. 3. To achieve the largest tuning range with the narrowest-band mirror coating required, the e-wave is resonated with the crystal angle typically below about 55°. Because the signal and pump waves are orthogonally polarized, the nonlinear crystal is AR coated at normal cut rather than at Brewster angle with no coating. The disadvantage is that, with Type-II interaction and with the pump and signal waves orthogonally polarized, the Poynting vectors of the two waves are not collinear for collinear phase-matching condition, thus leading to walk-off of the two waves. However, it was found experimentally [11] that the OPO prefers to match the Poynting vectors with slightly noncollinear interaction. This explains the small angle between the pump beam and signal beam directions shown in the schematic.

Ring- and linear-cavity configurations of both the pump laser and the OPO cavities have been tried. The relative advantages of the different configurations are as follows. For the pump laser, while the linear cavity is easier to operate, the ring cavity is less sensitive to the light reflected back from the OPO; thus, the two cavities are decoupled without the need for an isolator. In fact, the shortest pulse was achieved with the ring cavity (57 fs, see Fig. 4 for autocorrelation). For the OPO, the linear cavity has two

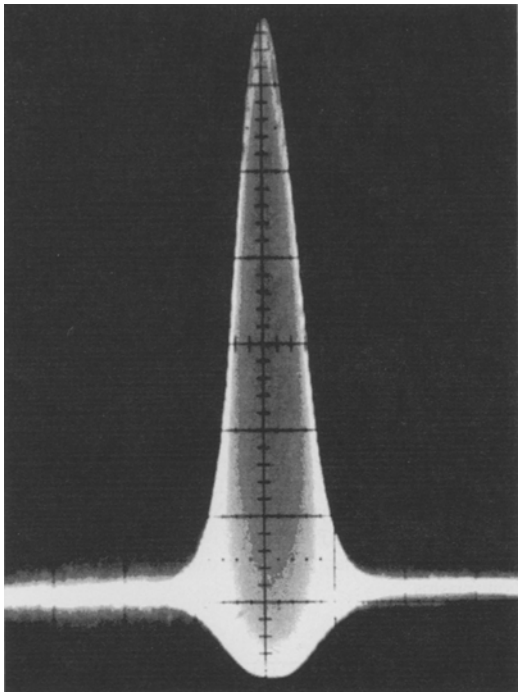

Fig. 4. Autocorrelation trace of 57 fs generated in a fs OPO with a ring cavity

advantages. It is easier to move the two intracavity prism compensators into and out of the cavity without the need for realigning all the mirrors. Only the output coupler needs to be retouched typically. Furthermore, with the linear-cavity configuration, it is possible to couple back the residual pump beam for a second pass to provide additional pumping. The disadvantage is that for single pass pumping, the signal pulse sees gain only in one direction but has Fresnel loss and additional group-velocity dispersion while traversing the crystal in the unpumped direction. With the ring-cavity for the OPO, the signal pulse sees gain each time it passes through the nonlinear crystal in synchronism with the pump pulse. In all cases, with intracavity prisms to compensate for group velocity dispersion, nearly perfect unchirped transform-limited pulses were obtained.

A major consideration in the design of femtosecond OPO is the inverse-pulse group-velocity mismatch in the three (pump, signal, and idler) very different wavelengths within the nonlinear crystal. This limits the crystal length to ≈ 1 mm for most inorganic nonlinear crystals. For such a short crystal, the spontaneous parametric emission that can be used for initial alignment purposes is generally quite low, on the order of 10^{-12} W in a 1 nm bandwidth. This together with the low single-pass gain makes length adjustment and alignment process rather difficult. With practice and experience, it can, however, be done routinely.

The striking features of the Ti:Sapphire-Pumped KTP OPO are: 1) The output power of the OPO is surprisingly high. A total of nearly 1 W of signal and idler power was obtained with nearly 55% of pump depletion. 2) Synchronized short pulses at seven wavelengths can be obtained simultaneously, including the residual pump, the signal, the idler, the non-phase-matched second harmonics of the signal and the idler, the sum of the pump and signal, and of the pump and the idler. Both the high power and the simultaneous output at multiple wavelengths offer an unprecendented opportunity for experimental sutdies of ultrafast process.

Tuning of the OPO could be achieved through several means. Certain amount of tuning can be achieved by simply varying the OPO cavity length. Because of group-velocity dispersion, the wavelength of the OPO will shift with the cavity length to keep the round-trip time of the signal pulse constant to match the fixed pump-pulse repetition rate. Tuning can of course be achieved by tuning the pump wavelength. One practical advantage of this tuning scheme is that only length adjustment of the OPO cavity is required. This is particularly important for noncritically phase-matched OPO in which the phase-matching condition is satisfied along a principal axis of the nonlinear crystal and, thus, less critical to angular misalignment. For larger tuning range, the phase-matching condition must be altered through changing either the orientation or the temperature of the crystal. Temperature tuning also has the advantage of not requiring any mechanical change in the OPO cavity to maintain noncritical phase-matching, for example.

The phase-matching bandwidth at, for example, a signal wavelength of 1.3 μm and a pump wavelength of 800 nm is on the order of 280 nm-mm for KTP and KTA and a little less for CTA. Because the parametric process is an elementary three-photon process, there is no energy storage in the cavity and the pulse width of the signal is primarily determined by that of the pump. Thus, potentially the pulse width can be down to the 20 fs range with sufficiently short pump pulses.

With intracavity dye laser pumping [8–10], when the OPO is properly adjusted to the near zero Group-Velocity Dispersion (GVD) point, the output characteristics are generally quite ideal with a smooth and relatively symmetric spectrum and very clean interferometric autocorrelation trace. It shows a close-to-ideal 8:1 ratio indicating good mode locking, an extremely flat background level indicating pulse-amplitude stability and lack of structure in the wings, indicative of chirp-free operation. With Ti-Sapphire-Laser pumping [15] at a much higher intensity level, the OPO pulses are characterized by a chirped and an unchirped regime. The chirped regime is encountered when the cavity is operated with a net positive GVD, and the unchirped regime occurs with net negative GVD. With intracavity dispersion compensation it is possible to vary the GVD from net negative values to net positive values. We observed a flip from chirped pulses to unchirped pulses as we changed from negative to net positive GVD. Near the 0 GVD point the pulses spontaneously jump between chriped and unchirped pulses, leading to instability in the pulse train. In the unchirped regime, highly stable operation of the OPO with ideal interferometric autocorrelation at close to 8:1 ratio (Fig. 4) can be obtained routinely.

2.2 Ti:*Sapphire-Laser* KTA *and* CTA *Femtosecond* OPO*s*

With the demonstration of the KTP fs OPO, it is obvious that many other nonlinear crystals could be used in fs parametric oscillators for other wavelength ranges and to

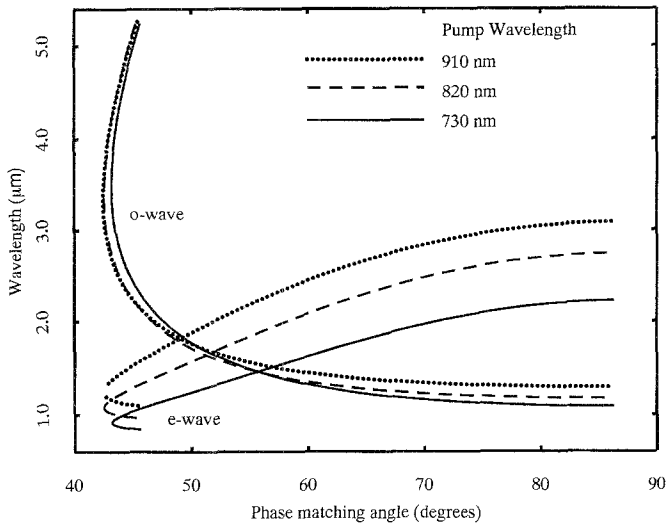

Fig. 5. Tuning curve of Ti:Sapphire-laser pumped Type-II phase-matched KTA femtosecond OPO

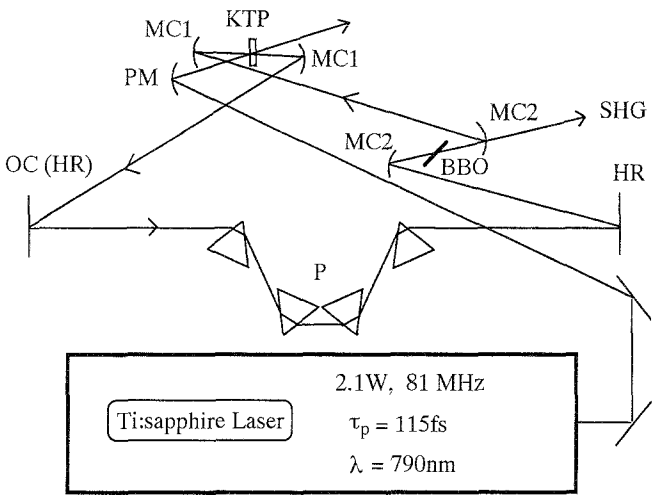

Fig. 7. Schematic of BBO intracavity doubled KTP fs OPO

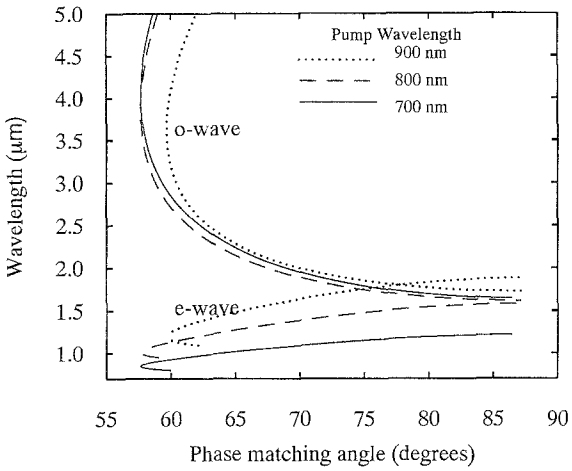

Fig. 6. Tuning curve of Ti:Sapphire laser pumped Type-II phase-matched CTA femtosecond OPO

meet other requirements. fs OPO using two other closely related crystals in the KTP isomorphs $MTiOXO_4$ where $M = MH_4$, K, Cs (for $X = As$ only), Rb, Tl, etc. and $X = P$ or As have already been successfully demonstrated. KTA [17] and CTA [18] are similar to KTP with one important difference. KTP has a rather strong absorption band due to the orthophosphate overtone near 3.5 μm which prevents the fs OPO to operate efficiently in the important 3–4 μm range. This overtone absorption band can be eliminated by replacing the phosphate with the heavier orthoarsenate $(AsO_4)^{-3}$ group. Both KTA and CTA can cover the 3–5 μm spectral range with comparable characteristics as those of the KTP fs OPO. The corresponding tuning curves of these OPOs are shown in Figs. 5 and 6.

2.3 *Intracavity-Doubled Femtosecond* OPO

For extension of the output of the fs lasers and the Ti:Sapphire laser pumped fs OPOs to the visible and to the ultraviolet, a variety of harmonic or sum-frequency generation processes can be used. One can use intracavity or external cavity doubling or summing of the output of the OPO, or the doubled or tripled output of a laser as the pump source for the OPO. Some of these have already been demonstrated with impressive results. Particularly successful examples are the intracavity BBO-doubled Rh 6G dye laser to 315 nm [19], the Ti:Sapphire laser to the blue [20], and the KTP OPO [21] to cover most of the visible-to-near IR range.

The key issue in frequency doubling of the femtosecond sources is the need to avoid broadening of the femtosecond pulses at the fundamental wavelength and the second-harmonic wavelength. This requires that the doubling crystal be very thin. For very thin crystals, the single-pass conversion efficiency is invariably very low even with very tight focusing, which means that intracavity doubling is often necessary. Because of its UV transparency and phase-matching properties, the crystal of choice for this purpose is β-Barium Borate (BBO).

In the experiment on intracavity-doubled KTP fs OPO reported in [20], an intracavity BBO crystal with a thickness of 47 μm was used. A schematic of such an arrangement is shown in Fig. 7. An additional focus to accommodate the BBO crystals is introduced into the OPO ring cavity. A ring cavity rather than a linear cavity is used in this case so that the OPO would oscillate in one direction and a single unidirectional second-harmonic beam is emitted. Due to the BBO crystals' large Second-Harmonic Generation (SHG) phase-matching bandwidth around the zero group-velocity mismatch point at 1.47 μm, tuning the frequency-doubled OPO output in the range of ≈1.1 to ≈1.6 μm (SHG ≈550 nm to ≈800 nm) requires no adjustment of the BBO phase-matching angle. Continuous tuning of the SHG from 550 nm to 660 nm limited only by optics available at the time of the experiment has been demonstrated (Fig. 8 shows data from 580 nm to 660 nm). Potential tuning range is from ≈500 nm to beyond 0.7 μm where the KTP fs OPO kicks in. The second-harmonic pulse train exhibits excellent stability, and as demonstrated by the real-time interferometric autocorrelation the pulses are chirp-free. Regardless of the transverse mode structure of the Ti:Sapphire pump laser,

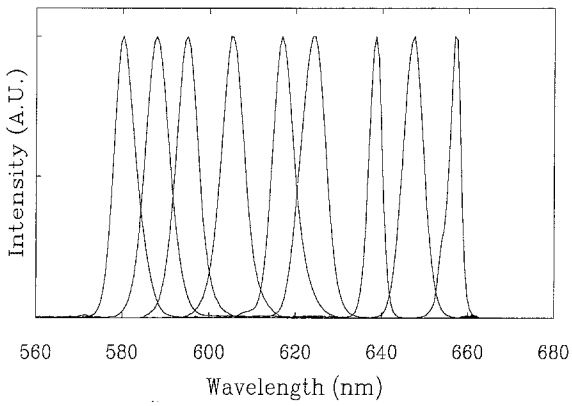

Fig. 8. Spectra of intracavity-doubled KTP OPO output

one can achieve an exceptionally clean TEM_{00} mode for the OPO which is imparted to the intracavity frequency-doubled beam.

Acknowledgements. This work was supported by JSEP and the National Science Foundation.

References

1. See the discussions in, for example, A.J. Taylor, D.J. Erskine, C.L. Tang: J. Opt. Soc. Am. B **2**, 663 (1985)
C.L. Tang, F.W. Wise, I.A. Walmsley: Rev. Phys. Appl. **22**, 1695 (1987)
F. Wise, M.J. Rosker, G.L. Millhauser, C.L. Tang: IEEE J. QE-**23**, 1116 (1987)
2. N. Kroll: Phys. Rev. **127**, 1207 (1972)
3. S.A. Akhmanov, R.V. Khokholov: Sov. Phys. JETP **16**, 252 (1963)
4. J.A. Giordmaine, R.C. Miller: Phys. Rev. Lett. **14**, 973 (1965)
5. See, for examples, the review articles by R.L. Byer: Optical parametric oscillators, in *Nonlinear Optics* Treatise in Quantum Electronics, Vol. 1, Part B, ed. by H. Rabin, C.L. Tang (Academic, New York 1975)
6. A. Laubereau, L. Greiter, W. Kaiser: Appl. Phys. Lett. **25**, 87 (1974)
H. Graener, A. Laubereau: App. Phys. B **29**, 213 (1982)
7. R. Danelyus, A. Piskarskas, V. Sirutkaitis: Sov. J. Quant. Electron. **12**, 1626 (1982)
A. Piskarskas, V. Smil'gyavichyus, A. Umbrasas: Sov. J. Quantum Electron. **18**, 155 (1988)
8. D.C. Edelstein, E.S. Wachman, C.L. Tang: Appl. Phys. Lett. **54**, 1728 (1989)
9. E.S. Wachman, D.C. Edelstein, C.L. Tang: Opt. Lett. **15**, 136 (1990)
10. E.S. Wachman, D.C. Edelstein, C.L. Tang: J. Appl. Phys. **70**, 1893 (1991)
11. D.E. Spence, P.N. Kean, W. Sibbett: Opt. Lett. **16**, 42 (1991)
12. J.Y. Zhang, J.Y. Huang, Y.R. Shen, C.T. Chen, B. Wu: Appl. Phys. Lett. **58**, 213 (1991)
13. G.P. Banfi, R. Danielius, A. Piskarskus, P. Di Trapani, P. Foggi, R. Roghini: Opt. Lett. **18**, 633 (1993)
14. A. Nebel, C. Fallnich, R. Beigang: CLEO/QELS '93, Baltimore, MD (May 1993) paper JWB5
15. W.S. Pelouch, P.E. Powers, C.L. Tang: Opt. Lett. **17**, 1070 (1992)
16. Q. Fu, G. Mak, H. Van Driel: Opt. Lett. **17**, 1006 (1992)
17. P.E. Powers, S. Ramakrishna, C.L. Tang, L.K. Cheng: CLEO 93, Baltimore, MD (May, 1993), paper CTHK2; Opt. Lett. **18**, 1171 (1993)
18. P.E. Powers, C.L. Tang: Opt. Lett. (in press)
19. D.C. Edelstein, E.S. Wachman, C.L. Tang: Appl. Phys. Lett. **52**, 2211 (1988)
20. R.J. Ellingson, C.L. Tang: Opt. Lett. **17**, 343 (1992)
21. R.J. Ellingson, C.L. Tang: Opt. Lett. **18**, 438 (1993)